Article
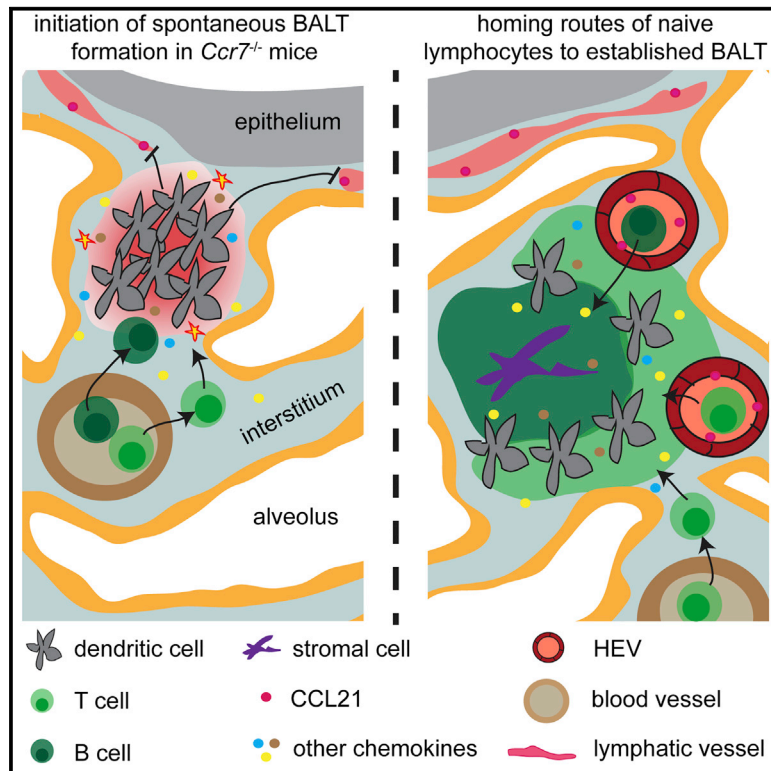
Manifold Roles of CCR7 and Its Ligands in the Induction and Maintenance of Bronchus-Associated Lymphoid Tissue

Graphical Abstract

Authors

Henrike Fleige, Berislav Bosnjak, Marc Permanyer, ..., Gerd Sutter, Sanjiv A. Luther, Reinhold Förster

Correspondence

foerster.reinhold@mh-hannover.de

In Brief

Fleige et al. demonstrate that CCR7 and its ligands CCL19, CCL21-serine, and CCL21-leucine orchestrate multiple steps during induction and maintenance of bronchus-associated lymphoid tissue (BALT) including DC-based initial developmental processes as well as homing of blood-derived lymphocytes via HEVs to established BALT.

Highlights

- Blood-derived lymphocytes enter BALT via two independent routes

- CCR7-associated DC migration defects lead to spontaneous BALT formation

- Pulmonary CCL21-leucine alone maintains DC egress and prevents BALT formation

- Aberrant lymphocyte migration promotes enhanced BALT formation in *plt/plt* mice

Manifold Roles of CCR7 and Its Ligands in the Induction and Maintenance of Bronchus-Associated Lymphoid Tissue

Henrike Fleige,[1] Berislav Bosnjak,[1] Marc Permanyer,[1] Jasmin Ristenpart,[1] Anja Bubke,[1] Stefanie Willenzon,[1] Gerd Sutter,[2] Sanjiv A. Luther,[3] and Reinhold Förster[1,4,*]
[1]Institute of Immunology, Hannover Medical School, 30625 Hannover, Germany
[2]Institute for Infectious Diseases and Zoonoses, University of Munich LMU, 80539 Munich, Germany
[3]Department of Biochemistry, Center for Immunity and Infection, University of Lausanne, 1066 Epalinges, Switzerland
[4]Lead Contact
*Correspondence: foerster.reinhold@mh-hannover.de
https://doi.org/10.1016/j.celrep.2018.03.072

SUMMARY

The processes underlying the development and maintenance of tertiary lymphoid organs are incompletely understood. Using a Ccr7 knockout/knockin approach, we show that spontaneous bronchus-associated lymphoid tissue (BALT) formation can be caused by CCR7-mediated migration defects of dendritic cells (DCs) in the lung. *Plt/plt* mice that lack the CCR7 ligands CCL19 and CCL21-serine do not form BALT spontaneously because lung-expressed CCL21-leucine presumably suffices to maintain steady-state DC egress. However, *plt/plt* mice are highly susceptible to modified vaccinia virus infection, showing enhanced recruitment of immune cells as well as alterations in CCR7-ligand-mediated lymphocyte egress from the lungs, leading to dramatically enhanced BALT. Furthermore, we identify two independent BALT homing routes for blood-derived lymphocytes. One is HEV mediated and depends on CCR7 and L-selectin, while the second route is via the lung parenchyma and is independent of these molecules. Together, these data provide insights into CCR7/CCR7-ligand-orchestrated aspects in BALT formation.

INTRODUCTION

Tertiary lymphoid organs (TLOs) are highly organized lymphoid structures, develop at sites of infection or chronic immune stimulation, and have been shown to play crucial roles in the generation of local immune responses (Halle et al., 2009; Moyron-Quiroz et al., 2004). Typically, these structures are named according to the anatomical site of their occurrence, such as the bronchus-associated lymphoid tissue (BALT) in the lung. BALT is located adjacent to a bronchus and next to a vein and artery. BALT is organized similar to secondary lymphoid tissue consisting of B cell follicles, in which germinal centers can develop, and T cell areas harboring antigen-presenting cells as well as high endothelial venules (HEVs). HEVs are also found in

lymph nodes (LNs) and are the sites that allow homing of lymphocytes from the blood (Fleige et al., 2014; Sminia et al., 1989; Xu et al., 2003). Importantly, the majority of the interstitial lymphocytic infiltrations observed in pulmonary infection does not fulfil the locational criteria and are thus not considered as BALT.

In the lungs of naive mice, BALT is not detectable but it forms spontaneously in mice lacking the chemokine receptor CCR7 (Kocks et al., 2007). In that study, our group could demonstrate that a defect in homing of regulatory T cells rather than impaired B cell egress from the lung leads to the BALT formation.

Apart from the spontaneous development in *Ccr7*-deficient mice, BALT can also be induced by intranasal (i.n.) administration of viruses including modified vaccinia virus Ankara (MVA), murine herpes virus-68 (MHV-68), and influenza virus (Halle et al., 2009; Kocks et al., 2009; Moyron-Quiroz et al., 2004). Furthermore, repetitive inhalations of heat-killed bacteria (Fleige et al., 2014; Toyoshima et al., 2000) or of lipopolysaccharide (LPS) in newborn mice allow induction of BALT (Rangel-Moreno et al., 2011). In a previous study, we have identified two major signaling pathways of the chemokine/chemokine receptor network, CXCL13/CXCR5 and CXCL12/CXCR4, as key factors of the induction and maturation of BALT (Fleige et al., 2014). However, the functional relevance of these and other homeostatic chemokines for homing of immune cells into already established BALT remained unclear. Whereas it is widely accepted that homing of naive T cells to lymph nodes via HEVs is controlled by integrins, selectins, and chemokine receptors (Förster et al., 2008), little is known how lymphocytes home to TLO. Xu et al. (2003) have analyzed adhesion molecules expressed on HEVs present in spontaneous BALT of autoimmune-prone NOD mice and found that lymphocyte homing is mediated by L-selectin/PNAd, $\alpha_4\beta_1$ integrin/VCAM1, and the LFA-1 adhesion pathway whereas $\alpha_4\beta_7$ and MAdCAM are not involved. Similar roles for L-selectin and α_4 integrins have been suggested for human BALT associated with lung carcinoma (Kawamata et al., 2009). Some studies show the relevance of chemokine receptors, including CCR7, for trafficking of lymphocytes toward and within the lung (Bromley et al., 2005; Lo et al., 2003). However, the role of chemokine receptors and their ligands in lymphocyte homing to BALT have been addressed very rarely. Analyzing tumor-induced BALT in lung cancer patients revealed the expression of a set of chemokines (CCL17, CCL19, CCL21, CCL22,

CXCL13, and interleukin [IL]-16) and their respective receptors (CCR7, CCR4, and CXCR5) on BALT-infiltrating T cells (de Chai-semartin et al., 2011). Furthermore, pulmonary expression of CCR7 and CXCR5 ligands in induced BALT indicating their role in recruitment of T and B cells to BALT (Fleige et al., 2014; Ran-gel-Moreno et al., 2007). Even though it is presumed that HEVs, decorated with chemokines and integrin-ligands represent the potential entry route for naive lymphocytes to BALT in mice, this has not been experimentally addressed so far.

In this study, we present data showing the importance of CCR7-mediated immune cell trafficking for respiratory immuno-logical homeostasis. Disconnection of the CCR7-signaling cascade on dendritic cells (DCs) leads to the spontaneous forma-tion of BALT. Apparently, one remaining isoform of the CCR7 ligand, CCL21-leucine, expressed on pulmonary lymphatic vessels in *plt/plt* mice is sufficient to prevent spontaneous BALT formation in those mice. However, upon MVA stimulation, we observed increased frequencies of early lymphoid infiltrates and massive formation of BALT at d12 in *plt/plt* mice indicating, albeit indirectly, a crucial role for CCL21-serine in lymphocyte egress from the lung. Furthermore, CCR7 and its ligands are also involved in HEV-mediated homing of blood-derived lymphocytes to BALT, highlighting the essential impact of the CCR7-CCL19/21 axis in different aspects of BALT biology.

RESULTS

Two Routes for Lymphocyte Homing to BALT

We have shown before that naive CD4$^+$ and CD8$^+$ T cells accu-mulate in MVA-induced BALT following adoptive intravenous (i.v.) transfer (Halle et al., 2009) but their precise route of BALT entry had not been studied thus far. We hypothesized that HEVs in BALT might represent a prominent homing route for naive lymphocytes. To this end, BALT was induced in wild-type (WT) mice by a single intranasal dose of MVA. 12 days later, these mice received fluorescently labeled naive lymphocytes from C57BL/6 donors by i.v. injection. Immunohistological anal-ysis of lung frozen sections identified HEVs in MVA-induced BALT and also identified that adoptively transferred lymphocytes are about to enter BALT via HEVs 30 min after transfer (Fig-ure 1A). To further address whether HEVs represent an exclusive homing route for lymphocytes entering BALT from the circula-tion, we inhibited homing via HEVs by applying an anti-L-selectin antibody to the BALT-bearing mice. Subsequently, fluorescently labeled lymphocytes were transferred i.v., and cells that homed into BALT were analyzed after defined time intervals. We observed that anti-L-selectin treatment almost completely blocked lymphocyte homing to BALT within the first 30 min (Fig-ures 1B, left, and 1C) but showed no effect when analyzing cell positioning 4 hr after transfer (Figures 1B, right, and 1C) although homing to LN was still completely blocked at that time (Figures S1A–S1D). Many adoptively transferred cells were already found in the lung parenchyma near the BALT 30 min after transfer (Fig-ure S1E), suggesting that interstitial lymphocytes can effectively enter BALT independent of L-selectin. Importantly, similar re-sults were observed in MVA-induced BALT of *plt/plt* mice as well as spontaneous BALT of *Ccr7*$^{-/-}$ mice (Figures 1D and 1E). Together, these findings identify HEVs as a fast homing

route of blood lymphocytes to BALT and also indicate that lym-phocytes of the lung parenchyma have access to BALT, although our experimental set up was not suited to completely clarify the mechanism of HEV-independent homing to BALT.

We next tested whether the chemokine receptor CCR7, recog-nized as an important homing receptor of T cells and CXCR5, known to guide B cells to B cell follicles, contributes to BALT homing. Competitive homing of naive WT and *Ccr7*-deficient T cells revealed a striking impairment of *Ccr7*-deficient cells after 30 min but not after 24 hr of transfer (Figures 2A and 2B). These findings resemble results obtained with anti-L-selectin treatment of WT recipient mice (Figures 1B–1D). Of note, homing of *Cxcr5*-deficient B cells to BALT was not impaired at any time point investigated (Figures 2C and 2D). Likewise, we were not able to detect any differences in BALT homing between WT and *Ccr7*-defcient DCs, neither 30 min nor 24 hr after intratracheal transfer (Figures 2E and 2F).

We then asked whether the CCR7-independent homing mechanisms for lymphocytes to BALT rely on signaling via other chemokine receptors. To this end, we blocked signaling of all G$_{\alpha i}$-coupled receptors by treating cells with pertussis toxin (ptx) prior to i.v. transfer. 24 hr later, we found 3-fold more untreated than ptx-treated lymphocytes in the BALT (Figures 2G and 2H) indicating that chemokine receptors also contribute to the homing of interstitial lymphocytes into BALT. Although neither *Cxcr5*- nor *Ccr7*-deficiency alone had any effect on the 24 hr parenchymal BALT homing of lymphocytes (Figures 2B and 2D) *Cxcr5*$^{-/-}$*Ccr7*$^{-/-}$ lymphocytes were strongly impaired in homing into BALT with B cells being more affected than T cells (Figures 2I and 2J). These findings demonstrate that CCR7 and CXCR5 synergize in guiding B cells into BALT.

Egress of Lung DCs Prevents the Development of Spontaneous BALT

Based on previous results demonstrating that intratracheal (i.t.)-transferred *Ccr7*-deficient DCs are impaired in egressing from the lung parenchyma into lymphatic vessels (Hintzen et al., 2006) and DCs are essential for development and maintenance of BALT (GeurtsvanKessel et al., 2009; Halle et al., 2009), we tested the hypothesis that the spontaneously developing BALT found in *Ccr7*-deficient mice (Kocks et al., 2007) is caused by impaired egress of DCs from the lung parenchyma. To this end, we took advantage of CCR7 "knockout/knockin" mice (Wendland et al., 2011). In these mice, murine *Ccr7* has been replaced by human *CCR7* flanked by a floxed stop cassette. Thus, crossing these mice with mice expressing the recombi-nase Cre under cell-type-specific promotors allows the selective expression of a CCR7 receptor processing the binding of murine ligands. We analyzed and quantified spontaneous BALT in mice that neither express mouse nor human CCR7 (*Ccr7*$^{-/-}$ *CCR7*$^{stop/stop}$ will be referred as *CCR7*$^{stop/stop}$), mice that express only human CCR7 in CD4$^+$ T cells (*Ccr7*$^{-/-}$*CCR7*$^{+/+}$*Cd4-cre*$^+$ will be referred as T-*CCR7*$^{+/+}$) and mice that express only human CCR7 in CD11c$^+$ DCs (*Ccr7*$^{-/-}$*CCR7*$^{+/+}$*Cd11c-cre*$^+$ will be referred as DC-*CCR7*$^{+/+}$).

BALT is rarely present in WT mice (Figure 3A) but we identified a considerable number of BALT in *Ccr7*-deficient, *CCR7*$^{stop/stop}$, and T-*CCR7*$^{+/+}$ mice (Figures 3B–3D, top). Spontaneous BALT in
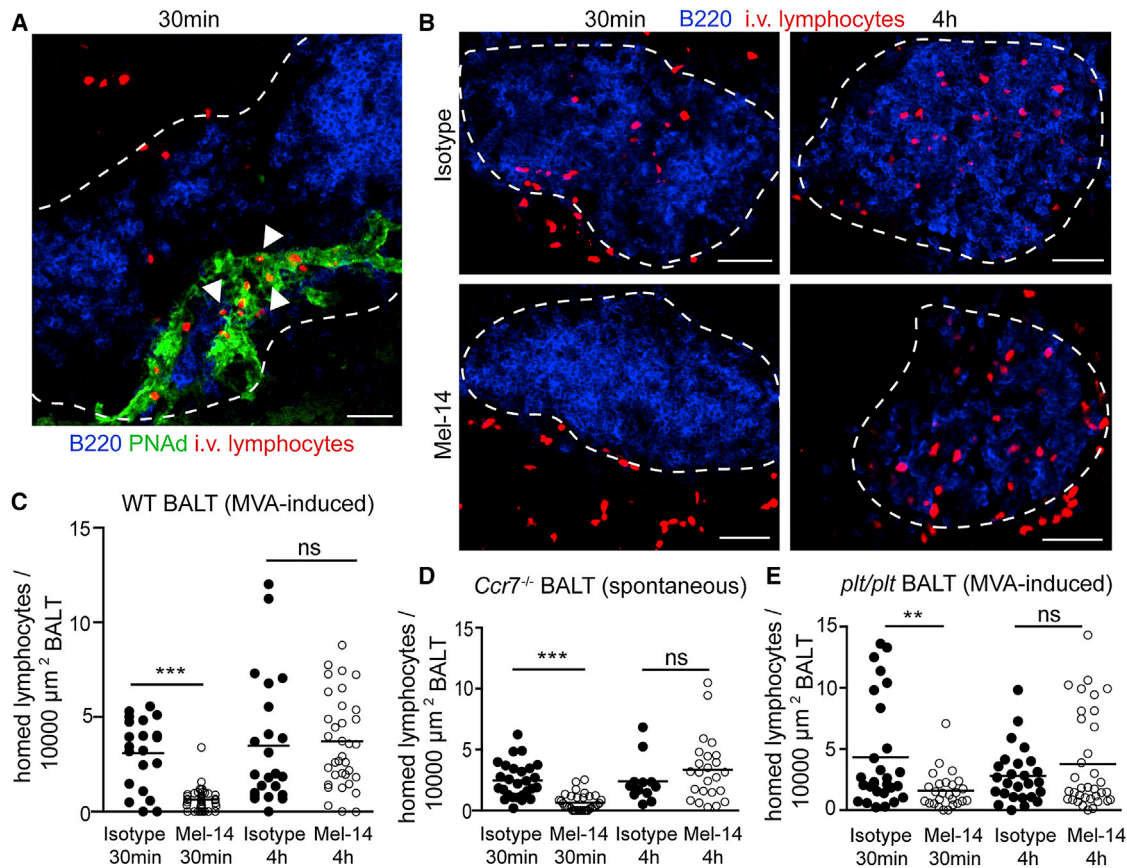
Figure 1. Naive Lymphocytes in the Blood Home to BALT via HEVs

(A and B) Immunofluorescence microscopy of lungs from 8- to 12-week-old C57BL/6 WT mice 12 days after i.n. administration of MVA. Mice were sacrificed either 30 min (A and B, left) or 4 hr (B, right) after i.v. transfer of TAMRA-labeled naive WT lymphocytes. Mice were untreated (A), treated i.p. with 250 μg anti-L-selectin antibody (Mel-14; B, bottom) or 250 μg isotype control (1H4; B, top). Frozen lung sections were stained with the antibodies indicated. Bars, 100 μm. Dashed lines define area of BALT. Arrowheads point to intravenously transferred lymphocytes, which are about to enter BALT via HEVs.

(C–E) Quantification of BALT-homed lymphocytes after i.v. transfer into anti-L-selectin (Mel-14)- or isotype-treated BALT-bearing WT (C), $Ccr7^{-/-}$ (D), or plt/plt (E) mice. Data are derived from at least two independent experiments with 5–8 mice and are represented as mean ± SD. ***p < 0.001; **p < 0.01; ns, not significant. See also Figure S1.

these mice is characterized by the presence of densely packed B cell follicles containing a network of CD21/35⁺ FDCs surrounded by T cells adjacent to a bronchus (Figures 3B–3D, bottom). Importantly, spontaneous BALT is largely absent in the lungs of DC-$CCR7^{+/+}$ mice (Figure 3E). Quantitative analysis revealed similar amounts of spontaneous BALT in $Ccr7$-deficient and $CCR7^{stop/stop}$ mice, a slight decrease in number and size in T-$CCR7^{+/+}$ mice, and an almost complete lack of spontaneous BALT in DC-$CCR7^{+/+}$ mice (Figures 3F and 3G). Together, these data suggest that impaired egress of DCs from the lung causes formation of spontaneous BALT in $Ccr7^{-/-}$ mice.

CCR7-Deficiency Does Not Interfere with the Development of MVA-Induced BALT

Because BALT develops spontaneously in $Ccr7$-deficient mice, and immune cells such as lymphocytes and DCs can home to BALT independently of CCR7, we hypothesized that MVA-induced BALT formation is not impaired in the absence of CCR7. To test this, we treated WT and $Ccr7$-deficient mice

with a single intranasal dose of MVA. 12 days after application, we observed BALT formation in WT, in $Ccr7$-deficient mice, and in selective $Ccr7$-proficient mice (Figures 4A–4D). While the number per section as well as the individual size of BALT was similar in WT, T-$CCR7^{+/+}$, and DC-$CCR7^{+/+}$ mice, both parameters were increased in $Ccr7$-deficient mice (Figures 4E and 4F). Together, these data indicate that $Ccr7$-deficiency does not interfere with MVA-induced BALT formation but leads to an increase in size and number of BALT structures.

Intact Trafficking of DCs Prevents the Formation of Spontaneous BALT in plt/plt Mice

The CCR7-CCR7L axis is also affected in plt/plt mice, a spontaneously occurring mutant in which the $Ccl19$ and the $Ccl21$-serine gene have been lost while the $Ccl21$-leucine gene is still present. Among other defects, plt/plt mice show impaired homing of T cells and DCs to secondary lymphoid organs and abnormalities in the localization of DCs within lymphoid organs (Gunn et al., 1999; Nakano et al., 1997, 1998). Interestingly, in contrast
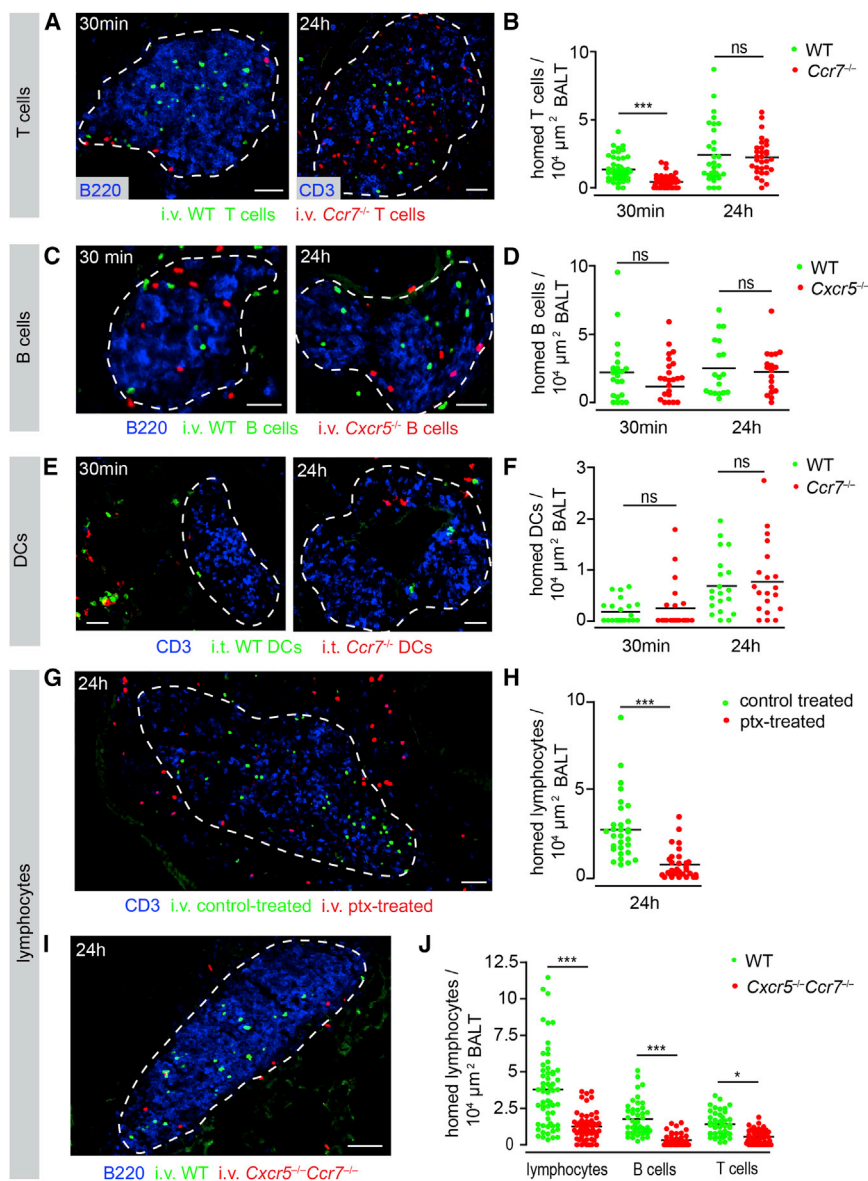
Figure 2. The Role of Chemokines during Lymphocyte Homing to BALT

(A, C, G, and I) Immunofluorescence microscopy of lungs from 8- to 12-week-old C57BL/6 WT mice either 30 min or 24 hr after simultaneous i.v. transfer of either WT and $Ccr7^{-/-}$ T cells (A), WT and $Cxcr5^{-/-}$ B cells (C), pertussis toxin (ptx) and control-treated lymphocytes (G), or WT and $Cxcr5^{-/-}Ccr7^{-/-}$ lymphocytes (I) into BALT-bearing WT mice. Transferred cells were fluorescently labeled. Frozen lung sections were stained with the antibodies indicated.

(B, D, H, and J) Quantification of BALT-homed T cells (B), B cells (D), or lymphocytes (H and J) 30 min or 24 hr after i.v. transfer. Data are derived from at least two independent experiments and are represented as mean ± SD. ***p < 0.001; *p < 0.05; ns, not significant.

(E) Immunofluorescence microscopy of BALT in the lungs of 8- to 12-week-old C57BL/6 WT mice either 30 min or 24 hr after simultaneous i.t. transfer of WT and $Ccr7^{-/-}$ DCs into BALT-bearing WT mice. Frozen lung sections were stained with the antibodies indicated.

(F) Quantification of BALT-homed WT and $Ccr7^{-/-}$ DCs 30 min or 24 hr after i.t. transfer. Data are derived from at least two independent experiments with 4–7 mice and are represented as mean ± SD; ns = not significant. Bars, 100 μm. Dashed lines define area of BALT.
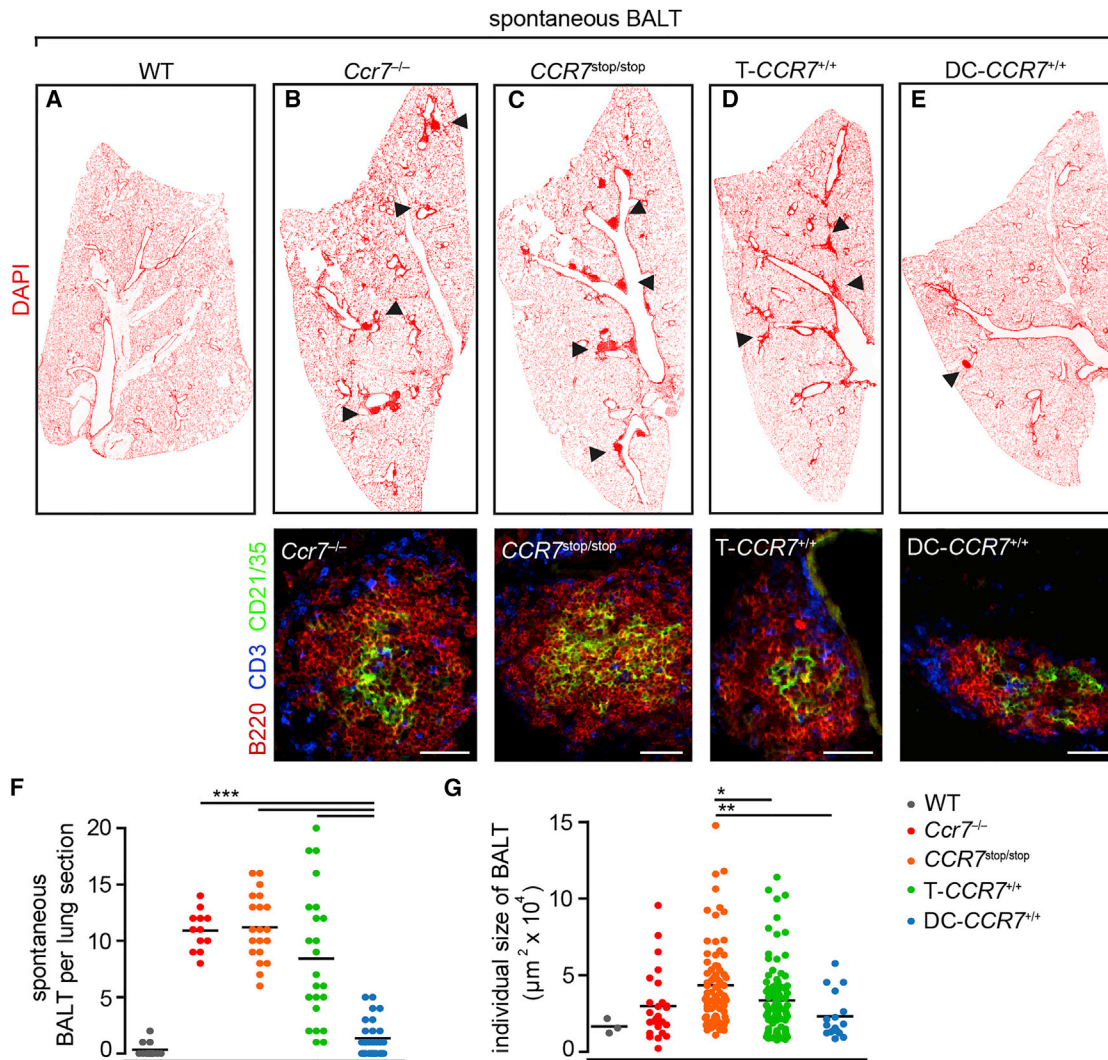
to $Ccr7$-deficient mice, we not only failed to detect spontaneous BALT but also any lymphoid infiltrations in the lungs of plt/plt mice (Figure 5A). An explanation for this unexpected finding could be that one isoform of CCL21 (CCL21-leucine) is still expressed on lymphatic vessels in non-lymphoid organs of plt/plt mice (Lo et al., 2003; Luther et al., 2000; Nakano and Gunn, 2001; Vassileva et al., 1999). Indeed, as described before (Jurisic et al., 2010; Kretschmer et al., 2013), we also observed CCL21 expression on CD90+ lymphatic vessels in the lungs of naive plt/plt mice (Figure 5B).

To analyze the migration defect of DCs in plt/plt mice, we i.t. transferred fluorescently labeled WT and $Ccr7$-deficient DCs into naive WT or plt/plt recipient mice. 24 hr after the transfer, we quantified transferred DCs in the lung as well as in the draining bronchial and the non-draining inguinal LN. As described earlier (Hintzen et al., 2006), in both WT and plt/plt

recipients significantly more $Ccr7$-deficient than WT DCs could be isolated from the lung (Figures 5C and 5D). When directly comparing the retention of WT DCs transferred in either WT or plt/plt recipients, we observed a slightly but not significantly higher number of DCs retained in the lungs of plt/plt mice (Figure 5E). Furthermore, while $Ccr7$-deficient DCs were completely excluded from the draining bronchial LN, WT DCs homed to this organ in WT and to a lower degree in plt/plt recip-

ients (Figure 5F). Neither WT nor in plt/plt recipients harbored any i.t. transferred DCs in non-draining inguinal LNs (Figure 5G).

Taken together, these data show that $Ccr7$-deficient DCs completely fail to egress from the lung while lung DCs of plt/plt mice only show a minor migratory defect to the lung draining LN most likely due to expression of CCL21-leucine. Although plt/plt mice never developed BALT, further histological analysis revealed that the salivary and lacrimal glands of these mice harbored considerable numbers of ectopic lymphoid structures. However, other organs that show tertiary lymphoid follicles in $Ccr7$-deficient mice, such as stomach and pancreas, were less severely or not at all affected in plt/plt mice (Figure S2). These findings might indicate a differential role of CCL21-leucine in DC migration and/or ectopic lymphoid organ formation across different organs.

spontaneous BALT

Figure 3. CCR7-Dependent Migratory Defects of DCs in the Lung Result in Spontaneous BALT Formation

(A–E) Immunofluorescence panoramic microscopy of naive lungs and detailed microscopy of spontaneous BALT of 8- to 12-week-old C57BL/6 WT (A), Ccr7^{−/−} (B), CCR7[stop/stop] (C), T-CCR7^{+/+} (D), or DC-CCR7^{+/+} (E) mice. Frozen lung sections were stained with the antibodies indicated. Arrowheads refer to individual spontaneous BALT. Bars, 100 μm.

(F and G) Number of spontaneous BALT per section and individual size of spontaneous BALT in WT, Ccr7^{−/−}, CCR7[stop/stop], T-CCR7^{+/+}, and DC-CCR7^{+/+} mice. Data are derived from at least two independent experiments with 3–7 mice and are represented as mean ± SD. *p < 0.05; **p < 0.01; ***p < 0.001. See also Figure S2.

MVA-Induced BALT Is Massively Enhanced in *plt/plt* Mice

To further address whether lack of CCL21-serine and CCL19 affects virus-induced BALT formation, we analyzed the lungs of *plt/plt* mice 12 days after intranasal MVA application. Surprisingly, we observed massive formation of induced BALT in those mice compared to WT (Figures 6A and 6B). Whereas in *plt/plt* mice almost three times more BALT was induced than in WT mice (*plt/plt*: 67.1 ± 19.8; WT: 25.0 ± 7.2; mean and SD), the individual BALT size was only slightly enhanced (Figures 6D and 6E).

We first speculated that this enormous BALT formation in *plt/plt* mice might result from a defect in egress of infiltrating lym-

phocytes because it had been suggested that CCR7 is involved in the egress of lymphocyte subsets from non-lymphoid tissue including the lung (Bromley et al., 2005; Debes et al., 2005). Given that CCL21-leucine is still expressed in the lung of *plt/plt* mice, we focused on the role of CCL19 in lymphocyte egress, the second ligand for CCR7 that is missing in *plt/plt* mice. Interestingly, we did not observe spontaneous BALT in CCL19-deficient mice (data not shown), and intranasal administration of MVA to those mice induced a similar number and size of BALT as in WT mice (Figures 6C–6E). These findings did not support our hypothesis for a relevant role of CCL19 in lymphocyte egress from the lung. Still, we cannot exclude that deficiency of CCL19 can be compensated by any of the two CCL21 isoforms.
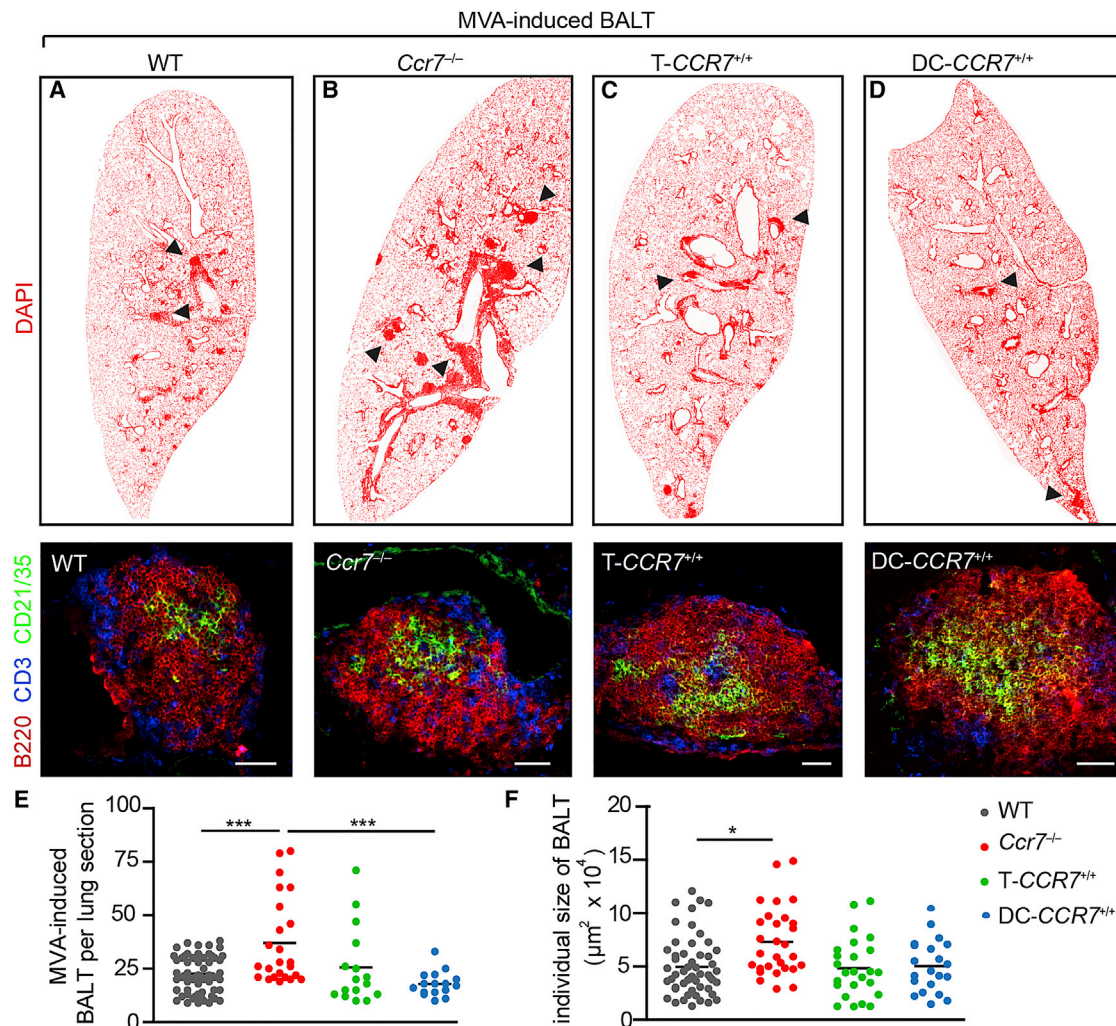
MVA-induced BALT

Figure 4. The Absence of CCR7 Does Not Interfere with the Development of MVA-Induced BALT

(A–D) Immunofluorescence panoramic microscopy of MVA-treated lungs and detailed microscopy of MVA-induced BALT of 8- to 12-week-old WT (A), $Ccr7^{-/-}$ (B), T-$CCR7^{+/+}$ (C), or DC-$CCR7^{+/+}$ (D) mice 12 days after i.n. administration of MVA. Frozen lung sections were stained with the antibodies indicated. Arrowheads refer to individual MVA-induced BALT. Bars, 100 μm.

(E and F) Number and individual size of MVA-induced BALT per section in WT, C$ccr7^{-/-}$, T-$CCR7^{+/+}$, and DC-$CCR7^{+/+}$ mice. Data are derived from at least two independent experiments with 4–16 mice and are represented as mean ± SD. *p < 0.05; ***p < 0.001.

To address this, we intratracheally transferred fluorescently labeled WT and, as control, $Ccr7$-deficient lymphocytes into either naive WT or plt/plt mice. 24 hr after the transfer, we quantified the number of lymphocytes being retained in the lung. In WT recipients, we observed significantly higher numbers of retained $Ccr7$-deficient lymphocytes compared to their WT counterparts (Figure 6F), consistent with previous data indicating that CCR7 is involved in the egress of lymphocyte subsets from the lung (Bromley et al., 2005; Debes et al., 2005). In contrast, in plt/plt recipients, we failed to detect any difference in the number of adoptively transferred WT or Ccr7-deficient lymphocytes remaining in the lung (Figure 6G) indicating that WT lymphocytes are equally impaired in leaving the lung as $Ccr7$-deficient cells. Direct comparison of transferred WT lymphocytes in either WT or plt/plt recipients revealed a significantly

increased number of lymphocytes being retained in lungs of plt/plt mice (Figure 6H). These data demonstrate that CCL21-serine and/or CCL19 are important for maintaining egress from the lung, with CCL21-leucine not being sufficient.

plt/plt Mice Are More Susceptible to MVA Infection and Show a Rapid and Enhanced Formation of BALT

Considering the regular MVA-induced BALT formation in $Ccr7$-deficient mice, the observed egress deficiency of lymphocytes from lungs of plt/plt mice cannot alone explain the massive induction of BALT upon MVA infection in these mice. We therefore performed a detailed comparative kinetic in BALT formation in WT and plt/plt mice using immunofluorescence microscopy. Interestingly, we observed a massive perivascular and peribronchiolar infiltration of T cells in plt/plt mice at day 3 after intranasal
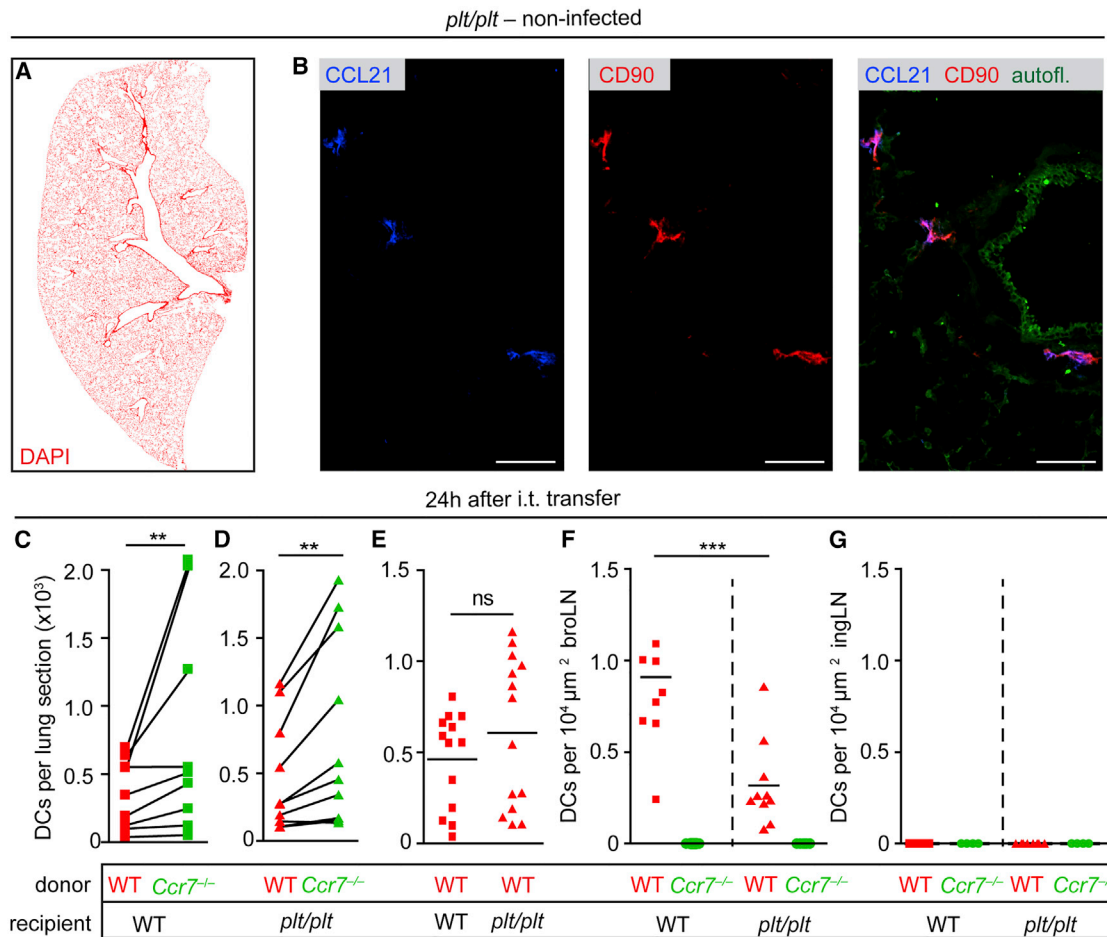
Figure 5. Intact Trafficking of DCs Prevents the Formation of Spontaneous BALT in *plt/plt* Mice

(A and B) Immunofluorescence panoramic (A) and detailed (B) microscopy of naive lungs from 8- to 12-week-old *plt/plt* mice. Frozen lung sections were stained with the antibodies indicated.

(C and D) Paired analysis of simultaneously transferred WT and *Ccr7−/−* DCs into untreated WT (C) or *plt/plt* (D) recipient mice 24 hr after i.t. transfer. Data are derived from two independent experiments with 5 mice and are represented as mean ± SD. **p < 0.01.

(E) Quantification of transferred WT DCs into untreated WT or *plt/plt* recipient 24 hr after i.t. transfer. Data are derived from two independent experiments with 5 mice; mean and SD. ns, not significant.

(F and G) Quantification of WT and *Ccr7−/−* DCs either detected in bronchial LN (broLN) (F) or inguinal LN (ingLN) (G) 24 hr after simultaneous i.t. transfer into either WT or *plt/plt* recipient mice. Data are derived from two independent experiments with 4–5 mice per group and are represented as mean ± SD. ***p < 0.001.

See also Figure S2.

MVA administration (Figure 7A). At day 6 after infection, B cell follicles have already been formed in *plt/plt* mice, whereas in WT mice, T cells have primarily been recruited to the lung, but these were still scattered diffusely around vessels and bronchioles (Figure 7B). In *plt/plt* mice, organized BALT characterized by separated T and B cell zones containing FDCs had been formed by day 8 (Figure 7C, not depicted) while at this time point, B cells just started to segregate toward the center of BALT in WT mice (Figure 7C). At day 12 after infection, large amounts of BALT had formed in *plt/plt* mice and displayed pronounced B cell follicles attended by T cells (Figure 7D). At the same time point, mature BALT defined by densely packed B cell follicles containing a network of FDCs (not depicted) surrounded by T cells was most abundantly present in WT mice (Figure 7D). Quantitative

analysis revealed that at any time point after MVA administration higher numbers of lymphoid infiltrates were present in *plt/plt* than in WT mice (Figure 7E, left). Furthermore, regardless of their organization or cellular composition, individual lymphoid infiltrates were larger in *plt/plt* mice (Figure 7E, middle), and as a consequence, the cumulative lymphoid size was higher in *plt/plt* mice at any time point analyzed (Figure 7E, right). Quantifying only mature BALT at day 12 after infection revealed three times more BALT in *plt/plt* compared to WT mice (Figure 7F). The high numbers of infiltrating T cells observed in *plt/plt* mice as early as at 3 days post infection (p.i.) raised the question whether *plt/plt* mice are more susceptible to intranasal MVA infection than WT mice. To answer this question we took advantage of a MVA reporter virus to visualize all infected cells (Kremer et al.,
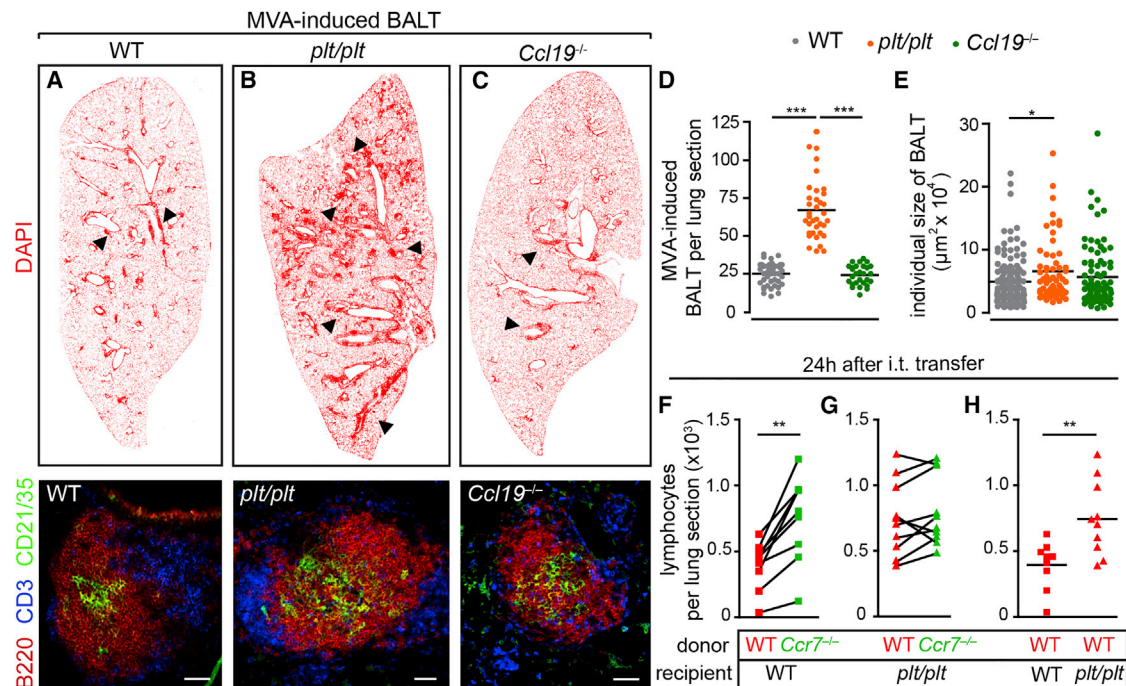
Figure 6. Massive Induction of MVA-Induced BALT in *plt/plt* Mice

(A–C) Immunofluorescence panoramic microscopy of MVA-treated lungs and detailed microscopy of MVA-induced BALT of 12- to 16-week-old WT (A), *plt/plt* (B), and *Ccl19*$^{-/-}$ (C) mice 12 days after i.n. administration of MVA. Frozen lung sections were stained with the antibodies indicated. Arrowheads refer to individual MVA-induced BALT. Bars, 100 μm.

(D and E) Number and individual size of MVA-induced BALT per section in WT, *plt/plt*, and *Ccl19*$^{-/-}$ mice. Data are derived from at least two independent experiments with 7–11 mice and are represented as mean ± SD. ***p < 0.001.

(F and G) Paired analysis of simultaneously transferred WT and *Ccr7*$^{-/-}$ lymphocytes into untreated WT (F) or *plt/plt* (G) recipient mice 24 hr after i.t. transfer. Data are derived from two independent experiments with 5 mice and are represented as mean ± SD. **p < 0.01.

(H) Quantification of transferred WT lymphocytes into untreated WT or *plt/plt* recipient 24 hr after i.t. transfer. Data are derived from two independent experiments with 5 mice and are represented as mean ± SD. **p < 0.01.
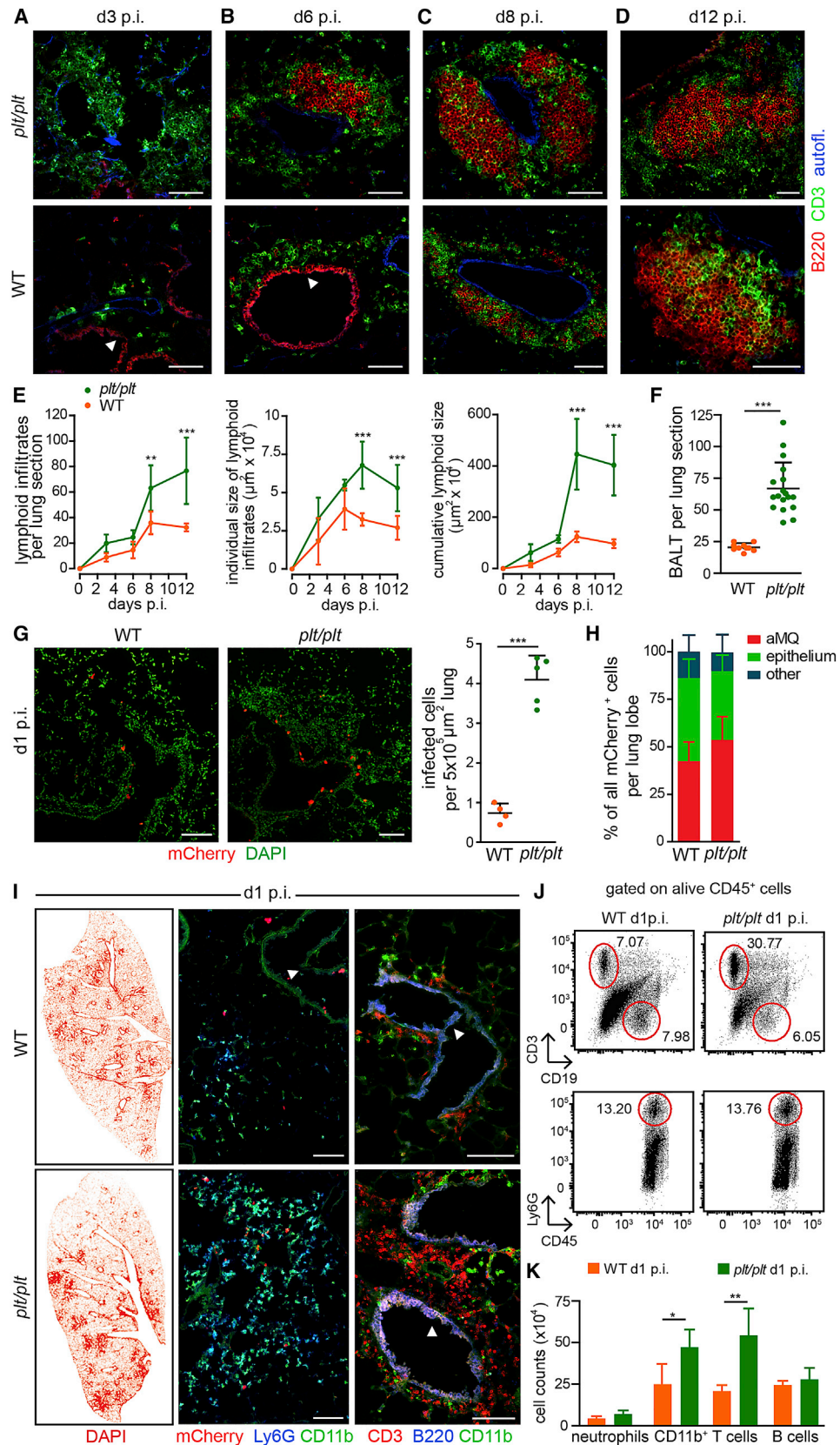
2012). Intranasal administration of MVA-mCherry identified four times more infected cells in lungs of *plt/plt* than in WT at d1 p.i. (Figure 7G). Further analysis of the cell types being infected revealed that alveolar macrophages, endothelial cells, as well as "other" not further-specified cells were equally more susceptible toward MVA infection in *plt/plt* relative to WT mice (Figure 7H). This increase in MVA susceptibility was paralleled by augmented immune cell recruitment to the lung of *plt/plt* mice as early as at day 1 p.i. (Figure 7I). Day 1 infiltrates in both WT and *plt/plt* mice primarily comprise of neutrophils, B cells, and T cells (Figures 7I–7K) with the latter being significantly enhanced in *plt/plt* mice.

DISCUSSION

The present study identified a multifaceted role of the chemokine receptor CCR7 and its ligands, CCL19 and CCL21 in the induction and maintenance of BALT. We show that lack of CCR7 on DCs but not T cells was responsible for spontaneous BALT formation in *Ccr7*$^{-/-}$ mice, and the pronounced accumulation of lymphocytes in BALT and lungs of *plt/plt* mice was caused by impaired lymphocyte egress most likely due to lack of CCL21-serine in these animals. Furthermore, this study identified 2 path-

ways that facilitate entry into BALT. One is directly from blood via high endothelial venules (HEV) and depends on L-selectin as well as CCR7/CCR7-ligands, whereas the second pathway is via the lung parenchyma and is independent of both signaling pathways.

Ectopic lymphoid tissues not only generate protective immune responses but are also suspected to the exacerbation of pathological immune-mediated processes. Therefore, a better understanding of the processes that regulate the continuous exchange of immune cells in tertiary lymphoid organs is needed. It is widely accepted for LNs that blood lymphocytes enter LNs via HEVs by a highly controlled multi-step adhesion cascade in which integrins as well as chemokines and their receptors orchestrate immune cell trafficking (Förster et al., 2008). Concerning the precise composition of homing molecules involved, this cascade shows some degree of organ specificity, thereby enabling certain subsets of leukocytes to migrate preferentially into their specific target tissue (Kunkel and Butcher, 2002). Similar to LNs, BALT is equipped with T cell areas harboring HEVs (Sminia et al., 1989) as well as postcapillary venules and lymphatic vessels. Although BALT clearly plays a role in pulmonary immunity, and lymphocytes are thought to home to BALT via HEVs, little is known about the multistep cascade that controls the migration

A d3 p.i.   **B** d6 p.i.   **C** d8 p.i.   **D** d12 p.i.

plt/plt

WT

B220   CD3   autofl.

E

● plt/plt
● WT

F

G   WT   plt/plt

d1 p.i.

mCherry DAPI

H

■ aMQ
■ epithelium
■ other

I   ——— d1 p.i. ———

WT

plt/plt

DAPI   mCherry Ly6G CD11b   CD3 B220 CD11b

J   gated on alive CD45⁺ cells

WT d1p.i.   plt/plt d1 p.i.

7.07   30.77

7.98   6.05

CD3

CD19

13.20   13.76

Ly6G

CD45

K

■ WT d1 p.i.   ■ plt/plt d1 p.i.

cell counts (x10⁴)

neutrophils   CD11b⁺   T cells   B cells

(legend on next page)

of lymphocytes to BALT. In this study, we now formally show that intravenously transferred lymphocytes home to MVA-induced BALT primarily via HEVs. We show that BALT homing via HEVs depends on L-selectin as well as on CCR7, and this route allows instantaneous entry of blood cells. However, our study also revealed a second port of entry into BALT that is independent of CCR7 and L-selectin and allows delayed homing of blood-derived immune cells via the lung parenchyma into BALT. Molecules involved in that homing route have not been addressed in this study. Furthermore, it remains unclear to what extent lymphocytes that have been primed in the lung-draining LN after MVA infection contributes to BALT formation. It has been shown before that activated lymphocytes can be efficiently recruited into inflamed tissue independent of CCR7 (Cupovic et al., 2016), but further studies are needed to clarify whether this is also the case for activated lymphocytes in MVA-induced BALT.

We reported earlier that *Ccr7*-deficient mice spontaneously develop BALT (Kocks et al., 2007) and now provide genetic evidence that deficiency of CCR7 on DCs impairs their spontaneous egress from the lung that ultimately leads to the formation of BALT in the lung. The accumulation of DCs in non-lymphoid areas has been correlated earlier with the formation of ectopic lymphoid tissue (Höpken et al., 2007), and the repetitive intratracheal transfers of bone-marrow-derived DCs to otherwise untreated mice resulted in BALT formation in WT mice (Geurts-vanKessel et al., 2009). These authors suggest a model by which DCs provide a continuous source of LTβ that recruits and retains B cells inside BALT in a CXCL13-dependent manner. Still, it remained unclear what kind of initial trigger leads to the initiation of BALT formation.

Here, we show that impaired steady-state egress of DCs from the lung is a sufficient trigger for BALT induction. *Ccr7*-knockout-knockin mice, in which CCR7 expression is restricted to DCs and allows them to regain their migratory capability, show efficient DC-homing to the draining LN, but not any spontaneous BALT formation. Along the same line, lungs of naive *plt/plt* mice that lack lymphoid CCL21-serine and CCL19 but express CCL21-leucine also do not develop spontaneous BALT. Although, CCR7-mediated DC egress from the lung is less efficient when only CCL21-leucine is present. Data of the present study provides circumstantial evidence that the CCR7-CCL21-leucine axis appears to be sufficient in preventing spontaneous tertiary lymphoid tissue formation in the lung. However, it is currently unclear whether this mechanism also prevents the spontaneous formation of ectopic lymphoid tissue in other organs. The observation that some but not all organs know to be targets of autoimmune diseases can spontaneously develop ectopic lymphoid follicles in *plt/plt* mice actually indicates a differential role of this chemokine across tissues in tertiary lymphoid tissue formation.

Still, *plt/plt* mice show a strong overreaction in BALT formation once this is induced by a virus such as MVA. We observed both increased BALT structures as well as larger individual BALT areas in *plt/plt* mice compared to WT mice. Enhanced airway inflammation has been reported in *plt/plt* mice before, as characterized by increased influx of eosinophils, higher levels of IL-4 and IL-13, combined with profound inflammation in peribronchiolar and perivascular areas compared to WT mice (Grinnan et al., 2006; Takamura et al., 2007; Xu et al., 2007; Yamashita et al., 2006). Moreover, BALT induction by mycobacterial and influenza infections in *plt/plt* mice has been reported before (Kahnert et al., 2007; Rangel-Moreno et al., 2007). However, contrary to our findings, those groups did not observe an enhanced formation or organization of BALT, but instead observed a regular or even impaired one. The reasons for these different observations are currently unclear, but it seems possible that this is due to the different pathogens used in these studies. Indeed, we have previously shown that different pathogens, such as MVA and *Pseudomonas aeruginosa*, both strong BALT inducers, used very different signaling pathways for induction of tertiary lymphoid organs (Fleige et al., 2014).

As mentioned above, it has been suggested before that CCR7 is involved in the egress of lymphocytes from non-lymphoid organs like skin or lung (Bromley et al., 2005; Debes et al., 2005). Interestingly, Grinnan et al. (2006) observed impaired exit of CD4^{+} and CD8^{+} T cells, but no egress defect of DC subsets, from the lungs in *plt/plt* mice. Along this line, we observed that DCs only show minor egress defects in *plt/plt* mice, whereas a large number of intratracheally transferred lymphocytes was retained in *plt/plt* lungs. It could be that mechanisms in addition to CCR7 direct lymphocytes from the lung to the draining LNs or that lymphocytes, but not DCs, rely on the presence of both

Figure 7. Early Enhanced Lymphoid Infiltrations upon MVA Infection in the Lungs of *plt/plt* Mice

(A–D) Immunofluorescence microscopy of lungs from 8- to 12-week-old *plt/plt* (top) and WT (bottom) mice 3 days (A), 6 days (B), 8 days (C), and 12 days (D) after i.n. MVA treatment. Frozen lung sections were stained with the antibodies indicated.

(E) Number, individual, and cumulative size of lymphoid aggregates per lung section in WT or *plt/plt* mice 3 days, 6 days, 8 days, and 12 days after i.n. MVA treatment. Data are derived from at least two independent experiments with 5–10 mice.

(F) Number of BALT per lung section in WT and *plt/plt* at day 12 after MVA treatment. Data are derived from three independent experiments with 6–10 mice.

(G) Immunofluorescence microscopy (left) and quantification of infected cells in the lungs from WT (left) and *plt/plt* (right) mice 1 day after infection with MVA-mCherry. Frozen lung sections were stained with DAPI. Data are derived from two independent experiments with 4–5 mice.

(H) Relative frequency of different cell types infected by MVA-mCherry 1 day after i.n. administration of WT and *plt/plt* mice. Data are derived from two independent experiments with 4–5 mice. aMQ, alveolar macrophage.

(I) Immunofluorescence panoramic (left) and detailed microscopy (right) of lungs from WT (top) and *plt/plt* (bottom) mice 1 day after i.n. administration of MVA. Frozen lung sections were stained with the antibodies indicated.

(J) Flow cytometry of single-cell suspensions of lungs from WT (left) and *plt/plt* (right) mice 1 day after i.n. administration of MVA using antibodies as indicated. Gate on all alive CD45^{+} cells.

(K) Absolute number of neutrophils, CD11b^{+} cells, T cells, and B cells in lungs of MVA-infected WT and *plt/plt* mice 1 day after administration. Data are representative for two independent experiments with 4–5 mice analyzed. Data are represented as mean ± SD. *p < 0.05; **p < 0.01; ***p < 0.001. Bars, 100 μm. Arrowheads indicate unspecific staining of vessels and bronchi that are also present in controls lacking primary antibodies.

isoforms of CCL21 and/or the presence of CCL19 on lymphatic vessels to efficiently leave the lung. Because the analysis of *Ccl19*-deficient mice did not reveal any abnormal retention of lymphocytes or enhanced levels of MVA-induced BALT, it seems that CCL21-serine is the essential factor that drives lymphocyte egress from lung. Another explanation could be the 1,000-fold higher sensitivity of DCs toward CCL21 and CCL19 compared to T cells resulting in more efficient exit from the lung, particularly if chemokines are limited (Kellermann et al., 1999).

Comparative kinetics in BALT-formation revealed profound differences between WT and *plt/plt* mice. It turned out that in *plt/plt* mice, both T cells and B cells are recruited much faster and organized BALT forms as early as at day 6 after MVA application. Furthermore, we found massive infiltrations of neutrophils in the early phase after infection in *plt/plt* lungs. The reason for the exaggerated immune reaction are currently unclear but are paralleled by our finding that 1 day p.i. *plt/plt* mice showed a 4-fold increase of infected cells in the lungs with alveolar macrophages and epithelial cells being equally affected. Because MVA cannot replicate in mammals, these observations demonstrate that *plt/plt* mice are more susceptible to the primary infection with MVA. This finding helps to explain the high amount of MVA-induced BALT found in these mice. Although the underlying molecular mechanism for this effect is unclear, it is unlikely that the deletion of CCL19 and CCL21-serine in *plt/plt* mice is directly responsible for increased susceptibility to MVA because neither CCL19 nor CCL21 showed any effect *in vitro* on MVA infection of alveolar macrophages (H.F., J.R., and R.F., unpublished data). Likewise, neither alveolar macrophages or epithelial cells, both targets for MVA, express CCR7 or CCR7 ligands. However, because the *plt/plt* mutation originally occurred in an outbred mouse strain, it cannot be excluded that genetic differences other than the deletion of the CCL19 and CCL21-serine locus in *plt/plt* mice trigger increased susceptibility to MVA infection. Clearly, further studies are needed to clarify this issue.

EXPERIMENTAL PROCEDURES

Mice
Mice were bred at a local animal facility or purchased from Charles River. $Ccr7^{-/-}$ mice (Förster et al., 1999), $Ccr7$ gene-targeted mice (Wendland et al., 2011), $Blr1^{-/-}$ ($Cxcr5$-deficient) mice (Förster et al., 1996), $Cxcr5^{-/-}Ccr7^{-/-}$ mice (Ohl et al., 2003), *plt/plt* mice (Nakano et al., 1998), and $Ccl19^{-/-}$ mice (Link et al., 2007) have been previously described. C57BL/6-*plt/plt* were produced by backcrossing of *plt/plt* mice (B6N:DDD-plt/Nkno B6.DDD-Ccl21bplt). All animals were maintained under SPF conditions and used at the age of 8–21 weeks. Both male and female mice were used throughout experiments in an equal manner. All experiments were performed in accordance with local animal welfare regulations reviewed by the institutional review board and the Lower Saxony State Office for Consumer Protection and Food Safety (TVV 12/0826, TVV 17/2568).

MVA
Recombinant MVA constructs have been described previously (Halle et al., 2016). In brief, MVA-mCherry were generated by homologous recombination using the plasmid vector pIIIdHR-P7.5 according to standard procedures (Kremer et al., 2012). For intranasal administration, mice were deeply anaesthetized with ketamine/xylazine, and 10^7 IU MVA diluted in 40 μL PBS was applied to the nostrils.

Immunohistology
For immunohistology, mice were perfused, organs embedded in Tissue-Tek OCT (Sakura), and frozen on dry ice. Fixed cryosections were rehydrated, blocked, and stained with different antibody "cocktails" at room temperature for 45 min.

Chemokine staining was performed by using a tyramide signal amplification (TSA) Cyanine 3 system (PerkinElmer).

Quantification of BALT
The amount of BALT was quantified as described before (Fleige and Förster, 2017). In brief, panoramic images of whole central sections of four different planes (close to main bronchi and vessels) per lung/mice were analyzed. Individual BALT structures were counted, measured, and the cumulative lymphoid size was calculated as the sum of all individual lymphoid structures present on one central lung section (polygon tool, cell'P/cellSens software, Olympus).

Isolation of Lungs and Flow Cytometry
Lungs from 8- to 14-week-old mice were perfused and digested for 60 min at 37°C. Red blood cells were lysed and single cell suspensions were blocked and incubated for 20 min on ice with different "cocktails" of antibodies. Finally, cells were washed and re-suspended with DAPI.

Adoptive Transfer of Lymphocytes
Either unsorted or magnetic-activated cell sorting (MACS) lymphocytes were isolated from spleen and LNs of C57BL/6 WT, $Ccr7^{-/-}$, $Cxcr5^{-/-}$, or $Cxcr5^{-/-}Ccr7^{-/-}$ mice and 1–5 × 10^7 fluorescently labeled cells were transferred i.v. into naive or BALT-bearing WT, $Ccr7^{-/-}$, or *plt/plt* recipients. 30 min, 4 hr, or 24 hr after the transfer, recipients were sacrificed, and the lung and LNs were harvested.

Blockade of L-selectin (CD62L) by *In Vivo* Administration of Anti-L-selectin Monoclonal Antibody
To block lymphocyte homing via HEVs, 250 μg anti-L-selectin monoclonal antibody (mAb) (Mel-14) or 250 μg isotype control (1H4) was given intraperitoneally (i.p.) into BALT-bearing mice 30 min before i.v. transfer of fluorescently labeled lymphocytes.

Blockade of $G_{\alpha i}$-Coupled Receptor Signaling by Incubation of Lymphocytes with Pertussis-Toxin
WT lymphocytes were incubated with 100 ng pertussis-toxin (ptx) or PBS in RPMI 1640 supplemented with 5% FCS and 10 mM HEPES for 4 hr at 37°C.

Generation of Bone-Marrow-Derived DCs
Bone-marrow-derived DCs were generated from bone marrow of C57BL/6 WT or $Ccr7^{-/-}$ mice by *in vitro* culture (Ohl et al., 2004).

Intratracheal Instillation
For intratracheal (i.t.) transfer into naive or BALT-bearing WT or *plt/plt* recipients, mice were anesthetized and a blunt cannula (0.7 × 19 mm, B. Braun) filled with 1–2 × 10^6 fluorescently labeled DCs or lymphocytes was instilled through the larynx into the trachea under visual control.

Statistical Analysis
Statistical analysis was performed with Prism 4 (Graph-Pad Software). When comparing two groups, significant values were determined using unpaired two-tailed t test. To compare multiple groups, one-way ANOVA was used. All error bars shown represent mean and SD. Statistical differences for the mean values are as follows: *$p < 0.05$; **$p < 0.01$; ***$p < 0.001$. All experiments shown were performed at least twice unless otherwise specified.

Detailed experimental procedures are included in the Supplemental Experimental Procedures.

SUPPLEMENTAL INFORMATION

Supplemental Information includes Supplemental Experimental Procedures and two figures and can be found with this article online at https://doi.org/10.1016/j.celrep.2018.03.072.

AUTHOR CONTRIBUTIONS

DECLARATION OF INTERESTS

The authors declare no competing interests.

REFERENCES

Bromley, S.K., Thomas, S.Y., and Luster, A.D. (2005). Chemokine receptor CCR7 guides T cell exit from peripheral tissues and entry into afferent lymphatics. Nat. Immunol. *6*, 895–901.

Cupovic, J., Onder, L., Gil-Cruz, C., Weiler, E., Caviezel-Firner, S., Perez-Shibayama, C., Rülicke, T., Bechmann, I., and Ludewig, B. (2016). Central nervous system stromal cells control local CD8(+) T cell responses during virus-induced neuroinflammation. Immunity *44*, 622–633.

de Chaisemartin, L., Goc, J., Damotte, D., Validire, P., Magdeleinat, P., Alifano, M., Cremer, I., Fridman, W.H., Sautès-Fridman, C., and Dieu-Nosjean, M.C. (2011). Characterization of chemokines and adhesion molecules associated with T cell presence in tertiary lymphoid structures in human lung cancer. Cancer Res. *71*, 6391–6399.

Debes, G.F., Arnold, C.N., Young, A.J., Krautwald, S., Lipp, M., Hay, J.B., and Butcher, E.C. (2005). Chemokine receptor CCR7 required for T lymphocyte exit from peripheral tissues. Nat. Immunol. *6*, 889–894.

Fleige, H., and Förster, R. (2017). Induction and analysis of bronchus-associated lymphoid tissue. Methods Mol. Biol. *1559*, 185–198.

Fleige, H., Ravens, S., Moschovakis, G.L., Bölter, J., Willenzon, S., Sutter, G., Häussler, S., Kalinke, U., Prinz, I., and Förster, R. (2014). IL-17-induced CXCL12 recruits B cells and induces follicle formation in BALT in the absence of differentiated FDCs. J. Exp. Med. *211*, 643–651.

Förster, R., Mattis, A.E., Kremmer, E., Wolf, E., Brem, G., and Lipp, M. (1996). A putative chemokine receptor, BLR1, directs B cell migration to defined lymphoid organs and specific anatomic compartments of the spleen. Cell *87*, 1037–1047.

Förster, R., Schubel, A., Breitfeld, D., Kremmer, E., Renner-Müller, I., Wolf, E., and Lipp, M. (1999). CCR7 coordinates the primary immune response by establishing functional microenvironments in secondary lymphoid organs. Cell *99*, 23–33.

Förster, R., Davalos-Misslitz, A.C., and Rot, A. (2008). CCR7 and its ligands: balancing immunity and tolerance. Nat. Rev. Immunol. *8*, 362–371.

GeurtsvanKessel, C.H., Willart, M.A., Bergen, I.M., van Rijt, L.S., Muskens, F., Elewaut, D., Osterhaus, A.D., Hendriks, R., Rimmelzwaan, G.F., and Lambrecht, B.N. (2009). Dendritic cells are crucial for maintenance of tertiary lymphoid structures in the lung of influenza virus-infected mice. J. Exp. Med. *206*, 2339–2349.

Grinnan, D., Sung, S.S., Dougherty, J.A., Knowles, A.R., Allen, M.B., Rose, C.E., 3rd, Nakano, H., Gunn, M.D., Fu, S.M., and Rose, C.E., Jr. (2006). Enhanced allergen-induced airway inflammation in paucity of lymph node T cell (plt) mutant mice. J. Allergy Clin. Immunol. *118*, 1234–1241.

Gunn, M.D., Kyuwa, S., Tam, C., Kakiuchi, T., Matsuzawa, A., Williams, L.T., and Nakano, H. (1999). Mice lacking expression of secondary lymphoid organ chemokine have defects in lymphocyte homing and dendritic cell localization. J. Exp. Med. *189*, 451–460.

Halle, S., Dujardin, H.C., Bakocevic, N., Fleige, H., Danzer, H., Willenzon, S., Suezer, Y., Hämmerling, G., Garbi, N., Sutter, G., et al. (2009). Induced bronchus-associated lymphoid tissue serves as a general priming site for T cells and is maintained by dendritic cells. J. Exp. Med. *206*, 2593–2601.

Halle, S., Keyser, K.A., Stahl, F.R., Busche, A., Marquardt, A., Zheng, X., Galla, M., Heissmeyer, V., Heller, K., Boelter, J., et al. (2016). In vivo killing capacity of cytotoxic T cells is limited and involves dynamic interactions and T cell cooperativity. Immunity *44*, 233–245.

Hintzen, G., Ohl, L., del Rio, M.-L., Rodriguez-Barbosa, J.-I., Pabst, O., Kocks, J.R., Krege, J., Hardtke, S., and Förster, R. (2006). Induction of tolerance to innocuous inhaled antigen relies on a CCR7-dependent dendritic cell-mediated antigen transport to the bronchial lymph node. J. Immunol. *177*, 7346–7354.

Höpken, U.E., Wengner, A.M., Loddenkemper, C., Stein, H., Heimesaat, M.M., Rehm, A., and Lipp, M. (2007). CCR7 deficiency causes ectopic lymphoid neogenesis and disturbed mucosal tissue integrity. Blood *109*, 886–895.

Jurisic, G., Iolyeva, M., Proulx, S.T., Halin, C., and Detmar, M. (2010). Thymus cell antigen 1 (Thy1, CD90) is expressed by lymphatic vessels and mediates cell adhesion to lymphatic endothelium. Exp. Cell Res. *316*, 2982–2992.

Kahnert, A., Höpken, U.E., Stein, M., Bandermann, S., Lipp, M., and Kaufmann, S.H.E. (2007). Mycobacterium tuberculosis triggers formation of lymphoid structure in murine lungs. J. Infect. Dis. *195*, 46–54.

Kawamata, N., Xu, B., Nishijima, H., Aoyama, K., Kusumoto, M., Takeuchi, T., Tei, C., Michie, S.A., and Matsuyama, T. (2009). Expression of endothelia and lymphocyte adhesion molecules in bronchus-associated lymphoid tissue (BALT) in adult human lung. Respir. Res. *10*, 97.

Kellermann, S.-A., Hudak, S., Oldham, E.R., Liu, Y.-J., and McEvoy, L.M. (1999). The CC chemokine receptor-7 ligands 6Ckine and macrophage inflammatory protein-3 β are potent chemoattractants for in vitro- and in vivo-derived dendritic cells. J. Immunol. *162*, 3859–3864.

Kocks, J.R., Davalos-Misslitz, A.C.M., Hintzen, G., Ohl, L., and Förster, R. (2007). Regulatory T cells interfere with the development of bronchus-associated lymphoid tissue. J. Exp. Med. *204*, 723–734.

Kocks, J.R., Adler, H., Danzer, H., Hoffmann, K., Jonigk, D., Lehmann, U., and Förster, R. (2009). Chemokine receptor CCR7 contributes to a rapid and efficient clearance of lytic murine gamma-herpes virus 68 from the lung, whereas bronchus-associated lymphoid tissue harbors virus during latency. J. Immunol. *182*, 6861–6869.

Kremer, M., Volz, A., Kreijtz, J.H.C.M., Fux, R., Lehmann, M.H., and Sutter, G. (2012). Easy and efficient protocols for working with recombinant vaccinia virus MVA. Methods Mol. Biol. *890*, 59–92.

Kretschmer, S., Dethlefsen, I., Hagner-Benes, S., Marsh, L.M., Garn, H., and König, P. (2013). Visualization of intrapulmonary lymph vessels in healthy and inflamed murine lung using CD90/Thy-1 as a marker. PLoS ONE *8*, e55201.

Kunkel, E.J., and Butcher, E.C. (2002). Chemokines and the tissue-specific migration of lymphocytes. Immunity *16*, 1–4.

Link, A., Vogt, T.K., Favre, S., Britschgi, M.R., Acha-Orbea, H., Hinz, B., Cyster, J.G., and Luther, S.A. (2007). Fibroblastic reticular cells in lymph nodes regulate the homeostasis of naive T cells. Nat. Immunol. *8*, 1255–1265.

Lo, J.C., Chin, R.K., Lee, Y., Kang, H., Wang, Y., Weinstock, J.V., Banks, T., Ware, C.F., Franzoso, G., and Fu, Y.X. (2003). Differential regulation of CCL21 in lymphoid/nonlymphoid tissues for effectively attracting T cells to peripheral tissues. J. Clin. Invest. *112*, 1495–1505.

Luther, S.A., Tang, H.L., Hyman, P.L., Farr, A.G., and Cyster, J.G. (2000). Coexpression of the chemokines ELC and SLC by T zone stromal cells and deletion of the ELC gene in the plt/plt mouse. Proc. Natl. Acad. Sci. USA *97*, 12694–12699.

Moyron-Quiroz, J.E., Rangel-Moreno, J., Kusser, K., Hartson, L., Sprague, F., Goodrich, S., Woodland, D.L., Lund, F.E., and Randall, T.D. (2004). Role of inducible bronchus associated lymphoid tissue (iBALT) in respiratory immunity. Nat. Med. *10*, 927–934.

Nakano, H., and Gunn, M.D. (2001). Gene duplications at the chemokine locus on mouse chromosome 4: multiple strain-specific haplotypes and the deletion of secondary lymphoid-organ chemokine and EBI-1 ligand chemokine genes in the plt mutation. J. Immunol. *166*, 361–369.

Nakano, H., Tamura, T., Yoshimoto, T., Yagita, H., Miyasaka, M., Butcher, E.C., Nariuchi, H., Kakiuchi, T., and Matsuzawa, A. (1997). Genetic defect in T lymphocyte-specific homing into peripheral lymph nodes. Eur. J. Immunol. *27*, 215–221.

Nakano, H., Mori, S., Yonekawa, H., Nariuchi, H., Matsuzawa, A., and Kakiuchi, T. (1998). A novel mutant gene involved in T-lymphocyte-specific homing into peripheral lymphoid organs on mouse chromosome 4. Blood *91*, 2886–2895.

Ohl, L., Henning, G., Krautwald, S., Lipp, M., Hardtke, S., Bernhardt, G., Pabst, O., and Förster, R. (2003). Cooperating mechanisms of CXCR5 and CCR7 in development and organization of secondary lymphoid organs. J. Exp. Med. *197*, 1199–1204.

Ohl, L., Mohaupt, M., Czeloth, N., Hintzen, G., Kiafard, Z., Zwirner, J., Blankenstein, T., Henning, G., and Förster, R. (2004). CCR7 governs skin dendritic cell migration under inflammatory and steady-state conditions. Immunity *21*, 279–288.

Rangel-Moreno, J., Moyron-Quiroz, J.E., Hartson, L., Kusser, K., and Randall, T.D. (2007). Pulmonary expression of CXC chemokine ligand 13, CC chemokine ligand 19, and CC chemokine ligand 21 is essential for local immunity to influenza. Proc. Natl. Acad. Sci. USA *104*, 10577–10582.

Rangel-Moreno, J., Carragher, D.M., de la Luz Garcia-Hernandez, M., Hwang, J.Y., Kusser, K., Hartson, L., Kolls, J.K., Khader, S.A., and Randall, T.D. (2011).

The development of inducible bronchus-associated lymphoid tissue depends on IL-17. Nat. Immunol. *12*, 639–646.

Sminia, T., van der Brugge-Gamelkoorn, G.J., and Jeurissen, S.H. (1989). Structure and function of bronchus-associated lymphoid tissue (BALT). Crit. Rev. Immunol. *9*, 119–150.

Takamura, K., Fukuyama, S., Nagatake, T., Kim, D.-Y., Kawamura, A., Kawauchi, H., and Kiyono, H. (2007). Regulatory role of lymphoid chemokine CCL19 and CCL21 in the control of allergic rhinitis. J. Immunol. *179*, 5897–5906.

Toyoshima, M., Chida, K., and Sato, A. (2000). Antigen uptake and subsequent cell kinetics in bronchus-associated lymphoid tissue. Respirology *5*, 141–145.

Vassileva, G., Soto, H., Zlotnik, A., Nakano, H., Kakiuchi, T., Hedrick, J.A., and Lira, S.A. (1999). The reduced expression of 6Ckine in the plt mouse results from the deletion of one of two 6Ckine genes. J. Exp. Med. *190*, 1183–1188.

Wendland, M., Willenzon, S., Kocks, J., Davalos-Misslitz, A.C., Hammerschmidt, S.I., Schumann, K., Kremmer, E., Sixt, M., Hoffmeyer, A., Pabst, O., and Förster, R. (2011). Lymph node T cell homeostasis relies on steady state homing of dendritic cells. Immunity *35*, 945–957.

Xu, B., Wagner, N., Pham, L.N., Magno, V., Shan, Z., Butcher, E.C., and Michie, S.A. (2003). Lymphocyte homing to bronchus-associated lymphoid tissue (BALT) is mediated by L-selectin/PNAd, alpha4beta1 integrin/VCAM-1, and LFA-1 adhesion pathways. J. Exp. Med. *197*, 1255–1267.

Xu, B., Aoyama, K., Kusumoto, M., Matsuzawa, A., Butcher, E.C., Michie, S.A., Matsuyama, T., and Takeuchi, T. (2007). Lack of lymphoid chemokines CCL19 and CCL21 enhances allergic airway inflammation in mice. Int. Immunol. *19*, 775–784.

Yamashita, N., Tashimo, H., Matsuo, Y., Ishida, H., Yoshiura, K., Sato, K., Yamashita, N., Kakiuchi, T., and Ohta, K. (2006). Role of CCL21 and CCL19 in allergic inflammation in the ovalbumin-specific murine asthmatic model. J. Allergy Clin. Immunol. *117*, 1040–1046.